6

Gas-Liquid Mass Transfer in an Unbaffled Vessel Agitated by Unsteadily Forward-Reverse Rotating Multiple Impellers

Masanori Yoshida[1], Kazuaki Yamagiwa[1],
Akira Ohkawa[1] and Shuichi Tezura[2]
[1]*Department of Chemistry and Chemical Engineering, Niigata University*
[2]*Shimazaki Mixing Equipment Co., Ltd.*
Japan

1. Introduction

Gas-sparged vessels agitated by mechanically rotating impellers are apparatuses widely used mainly to enhance the gas-liquid mass transfer in industrial chemical process productions. For gas-liquid contacting operations handling liquids of low viscosity, baffled vessels with unidirectionally rotating, relatively small sized turbine type impellers are generally adopted and the impeller is rotated at higher rates. In such a conventional agitation vessel, there are problems which must be considered (Bruijn *et al.*, 1974; Tanaka and Ueda, 1975; Warmoeskerken and Smith, 1985; Nienow, 1990; Takahashi, 1994): 1) occurrence of a zone of insufficient mixing behind the baffles and possible adhesion of a scale to the baffles and the need to clean them periodically; 2) formation of large gas-filled cavities behind the impeller blades, producing a considerable decrease of the impeller power consumption closely related to characteristics on gas-liquid contact, i.e., mass transfer; 3) restriction in the range of gassing rate in order to avoid phenomena such as flooding of the impeller by gas bubbles, etc. Neglecting these problems may result in a reduced performance of conventional agitation vessels. Review of the literatures for the conventional agitation vessel reveals that a considerable amount of work was carried out to improve existing type apparatuses. However, a gas-liquid agitation vessel which is almost free of the above-mentioned problems seems not to have hitherto been available. Therefore, there is a need to develop a new type apparatus, namely, an unbaffled vessel which provides better gas-liquid contact and which may be used over a wide range of gassing rates.

As mentioned above, in conventional agitation vessels, baffles are generally attached to the vessel wall to avoid the formation of a purely rotational liquid flow, resulting in an undeveloped vertical liquid flow. In contrast, if a rotation of an impeller and a flow produced by the impeller are allowed to alternate periodically its direction, a sufficient mixing of liquid phase would be expected in an unbaffled vessel without having anxiety about the problems encountered with conventional agitation vessels. We developed an agitator of a forward-reverse rotating shaft whose unsteady rotation proceeds while alternating periodically its direction at a constant angle (Yoshida *et al.*, 1996). Additionally,

we designed an impeller with four blades as are longer and narrower and are of triangular sections. The impellers were attached on the agitator shaft to be multiply arranged in an unbaffled vessel with a liquid height-to-diameter ratio of 2:1. This unbaffled vessel agitated by the forward-reverse rotating impellers was applied to an air-water system and then its performance as a gas-liquid contactor was experimentally assessed, with resolutions for the above-mentioned problems being provided (Yoshida *et al.*, 1996; Yoshida *et al.*, 2002; Yoshida *et al.*, 2005).

Liquid phases treated in most chemical processes are mixtures of various substances. Presence of inorganic electrolytes is known to decrease the rate for gas bubbles to coalesce because of the electrical effect at the gas-liquid interface (Marrucci and Nicodemo, 1967; Zieminski and Whittemore, 1971). In many cases, the electrical effect creates different gas-liquid dispersion characteristics, such as decreased size of gas bubbles dispersed in liquid phase without practical changes in their density, viscosity and surface tension (Linek *et al.*, 1970; Robinson and Wilke, 1973; Robinson and Wilke, 1974; Van't Riet, 1979; Hassan and Robinson, 1980; Linek *et al.*, 1987). The present work assesses the mass transfer characteristics in aerated electrolyte solutions, following assessment of those in the air-water system, for the forward-reverse agitation vessel. In conjunction with the volumetric coefficient of mass transfer as viewed from change in power input, which is a typical performance characteristic of gas-liquid contactors, the dependences of mass transfer parameters such as the mean bubble diameter, gas hold-up and liquid-phase mass transfer coefficient were examined. Such investigations including correlation of the mass transfer parameter could quantify enhancement of the gas-liquid mass transfer and predict reasonably the values of volumetric coefficient.

2. Experimental

2.1 Experimental apparatus

A schematic diagram of the experimental set-up is shown in Fig. 1. The vessel was a combination of a cylindrical column (0.25 m inner diameter, D_t, 0.60 m height) made of transparent acrylic resin and a dish-shaped stainless-steel bottom (0.25 m inner diameter and 0.075 m height). The liquid depth, H, was maintained at 0.50 m, which was twice D_t. An impeller is one with four blades whose section is triangular (0.20 m diameter, D_i, Fig. 2), and was used in a multiple manner where the triangle apex of the blade faces downward. Different experiments employed 2-8 impellers; the number is represented as n_i. The impellers were set equidistantly on the shaft in its section between the lower end of the column and the liquid surface. Additionally, the angular difference of position between the blades of one impeller and those of upper and lower adjacent impellers was 45 degree. In the mechanism for transmitting motion used here (Yoshida *et al.*, 2001), when the crank is rotated one revolution, the shaft on which the impellers were attached first rotates up to one-quarter of a revolution in one direction, stops rotating at that position and rotates one-quarter of a revolution in the reverse direction. That is, the angular amplitude of forward-reverse rotation, θ_o, is $\pi/4$. When such a rotation with sinusoidal angular displacement is expressed in the form of a cosine function, the angular velocity of impeller, ω_i, is given by the sine function as

$$\omega_i = 2\pi\theta_o N_{ff} \sin(2\pi N_{ff} t) \quad (1)$$

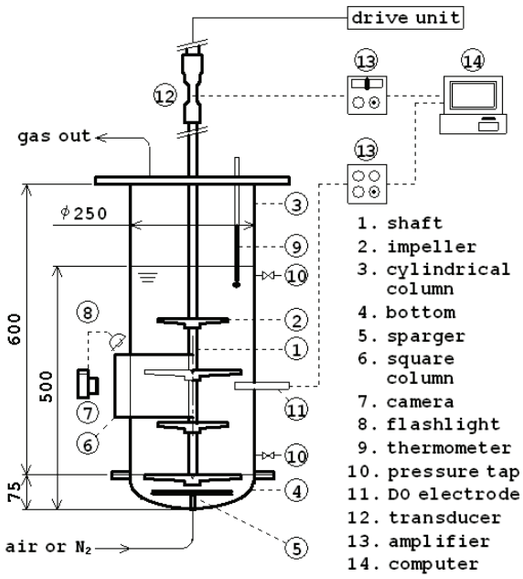

Fig. 1. Schematic flow diagram of experimental apparatus. Dimensions in mm.

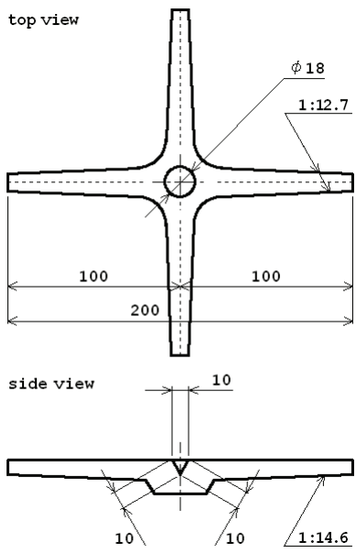

Fig. 2. Structure and dimensions (in mm) of the impeller used.

where N_{fr} is the frequency of forward-reverse rotation and was varied from 1.67 to 6.67 Hz as an agitation rate. A ring sparger with 24 holes of 1.2 mm diameter (the circle passing through the holes' centers is 0.16 m diameter) was used for aeration. The gassing rate ranged from 0.4×10^{-2} to 1.7×10^{-2} m/s in the superficial gas velocity, V_s. Comparative experiments in the unidirectional rotation mode of impeller were undertaken using a conventional impeller, a disk turbine impeller with six flat blades (DT, 0.12 m D_i). DTs were set in a dual configuration on the shaft and a nozzle sparger with a single hole of 7 mm diameter was equipped for the fully baffled vessel. Geometrical conditions such as D_t and H were common to the forward-reverse and unidirectional agitation modes. Sodium chloride

solutions of different concentrations (up to 2.0 wt%) were used at 298 K as the liquid phase containing electrolyte. Physical properties of these liquids such as density, ρ, viscosity, μ, and diffusivity, D_L, were approximated by those for water.

2.2 Measuring system for power consumption of impeller

A system measuring unsteady torque of the shaft due to unsteady rotation of the impeller consisted of the fluid force transducing part, impeller displacement transducing part and signal processing part. In the fluid force transducing part, the strain generated during operation in a copper alloy coupling having four strain gauges is recorded continuously. In the impeller displacement transducing part, a switching circuit composed of a light emitting diode and a phototransistor, etc. pulses the rest point in cycles of forward-reverse rotation of impeller, thereby adjusting the frequency of forward-reverse rotation and defining the trigger point of measurements as the rest point. In the signal processing part, the analog signals of voltage from the fluid force and impeller displacement transducers are input into a computer after being digitized to permit calculations of the torque of the forward-reverse rotating shaft. The fluid force transducer detects the strains caused by different forces such as fluid forces acting on the impeller and shaft and inertia forces due to the acceleration of the motions of the impeller and shaft. The fluid force acting on the shaft was found to be negligibly small in analysis, compared with that acting on the impeller. Hence, the moment of the fluid force acting on the impeller, i.e., the agitation torque, can be obtained by subtracting the value measured in air from that in liquid, with the impellers attached.

The time-course curve of instantaneous power consumption, P_m, was obtained by multiplying the instantaneous torque, T_m, measured over one cyclic time of forward-reverse rotation of impeller by the angular velocity of impeller at the corresponding time [Eq. (1)]. The time-averaged power consumption, $P_{m\mathrm{av}}$, that is based on the total energy transmitted in one cycle was graphically determined from the time-course curve of P_m.

$$P_{m\mathrm{av}} = \oint P_m \mathrm{d}t/(1/N_{fr}) = \Sigma P_m \Delta t/(1/N_{fr}) \tag{2}$$

The following equation was used to calculate the power consumption for aeration, P_a:

$$P_a = \rho g V_s V_\mathrm{o} \tag{3}$$

where g is the acceleration due to gravity and V_o is the liquid volume above the sparger.

2.3 Measuring system for mass transfer parameters

For mass transfer experiments, the physical absorption of oxygen in air by water was used. The volumetric coefficient of oxygen transfer was determined by the gassing-out method with purging nitrogen. The time-dependent dissolved oxygen concentration (DO), C_L, after starting aeration under a given agitation was measured at the midway point of the liquid depth, i.e., the distance 0.25 m above the vessel bottom, using a DO electrode. When there was assumed to be little difference of oxygen concentration between the inlet air and outlet gas, the overall volumetric coefficient based on the liquid volume, $K_L a_\mathrm{L}$, was obtained from the following relation:

$$\ln[(C_L^* - C_L)/(C_L^* - C_{L\mathrm{o}})] = -K_L a_\mathrm{L} t \tag{4}$$

where $C_{L\mathrm{o}}$ is the initial concentration, C_L^* is the saturated concentration and t is the time. The error in the value of volumetric coefficient due to the response lag of the DO electrode

was corrected based on the first-order model using the time constant obtained in response experiments. K_La_L determined in this way was regarded as the liquid-side volumetric coefficient, k_La_L, because in this system, the resistance to mass transfer on the gas side was negligible compared with that on the liquid side.

In analyzing the time-course of oxygen concentration, a model was used assuming well-mixed liquid phase and gas phase without depletion. Previous researchers including one (Calderbank, 1959) referred for comparison have resolved the difficulty to analyze changes in gas phase by ignoring the depletion of solute, so that gas bubbles are assumed to have the same composition between the inlet and outlet gas streams at all time. It has been demonstrated that the errors inherent in such assumptions are significant and that their effect on evaluation of the volumetric coefficient is considerable (Chapman *et al.*, 1982; Linek *et al.*, 1987), which may underestimate the values of volumetric coefficient. Justification for the assumptions lies in the fact that agreement between the observed values and calculated ones from earlier empirical equations (Van't Riet, 1979; Nocentini *et al.*, 1993) was satisfactory and that the analytical result still preserves the relative order of difference between the agitation modes, making them practical comparison. Therefore, it is to be noted that the values of volumetric coefficient evaluated in this work are confined to the control for comparison and would be required for the reliability to be improved.

Photographs of gas bubbles were taken at the midway point of the liquid depth, i.e., the distance 0.25 m above the vessel bottom. A square column was set around the vessel section where the photographs were taken. The space between the square column and vessel was also filled with water to reduce optical distortion. A point immediately inside the vessel wall was focused on. When a lamp light was collimated through slits to illuminate the vertical plane including that point, bodies within 25 mm inside the vessel wall could be almost in focus. The average value of readings of a scale placed in that space was employed as a measure for comparison. A spheroid could approximate the bubble shape observed on the photographs. By measuring the major and minor axes for at least 100 bubbles photographed, the volume-surface mean diameter, d_{vs}, was calculated. The overall gas hold-up, ϕ_{gD}, based on the gassed liquid volume was determined using the manometric technique (Robinson and Wilke, 1974). The manometer reading was corrected for the difference of dynamic pressure, namely, that of the reading measured in ungassed liquid. When the dispersion is assumed to comprise spherical gas bubbles of size d_{vs}, the gas-liquid interfacial area per unit volume of gassed liquid, a_D, is calculated from the following equation:

$$a_D=6\phi_{gD}/d_{vs} \tag{5}$$

The liquid-phase mass (oxygen) transfer coefficient, k_L, was separated from the volumetric coefficient based on the liquid volume, k_La_L, using a_D and ϕ_{gD}.

$$k_L=(k_La_D)/a_D=(k_La_L)(1-\phi_{gD})/a_D \tag{6}$$

3. Power characteristics of forward-reverse agitation vessel

3.1 Viscous and inertial drag coefficients

The following expression is assumed for the torque of the forward-reverse rotating shaft on which the impellers were attached, i.e., the agitation torque, T_m:

$$T_m=C_d\rho D_i^5\omega_t|\omega_t|+C_m\rho D_i^5(\mathrm{d}\omega_t/\mathrm{d}t) \tag{7}$$

where D_i is the diameter of impeller, ω_i is the angular velocity of impeller, ρ is the density of fluid around impeller and t is the time. C_d is the viscous drag coefficient relating to the moment of viscous drag on impeller and C_m is the inertial drag coefficient relating to the moment of inertia force due to the acceleration of fluid motion caused by impeller forward-reverse rotation. These coefficients are expressed in a form of average over one cyclic time of forward-reverse rotation of impeller as follows, respectively, using the coefficients of the fundamental frequency components of sine and cosine obtained by expanding Eq. (7), into which the time-dependence of ω_i [Eq. (1)] was substituted, in Fourier series:

$$C_d=(3\pi/8)[(1/\pi)\oint(T_m/\rho D_i^5\theta_o^2\omega_{fr}^2)\sin(\omega_{fr}t)\mathrm{d}(\omega_{fr}t)] \quad (8)$$

$$C_m=\theta_o[(1/\pi)\oint(T_m/\rho D_i^5\theta_o^2\omega_{fr}^2)\cos(\omega_{fr}t)\mathrm{d}(\omega_{fr}t)] \quad (9)$$

where ω_{fr} is the angular frequency of the sinusoidal time-course of ω_i and is equal to $2\pi N_{fr}$. Moreover, Eq. (7) for the time-course of T_m is rewritten as follows:

$$T_m=(\rho D_i^5\theta_o^2\omega_{fr}^2)[(8C_d/3\pi)\sin(\omega_{fr}t)+(C_m/\theta_o)\cos(\omega_{fr}t)] \quad (10)$$

The data of agitation torque, T_m, measured in electrolyte solutions of different concentrations when the gassing rate, the agitation rate and the number of impellers were varied were analyzed based on Eq. (10). An example of ungassed and gassed analytical results is shown in Fig. 3. The thin solid line in the figure is for the values calculated from Eq. (10) with the viscous and inertial drag coefficients, C_d and C_m, determined experimentally using Eqs (8) and (9). Good agreements were found between the observed and calculated values, regardless of the conditions with and without aeration. For the difference due to aeration, it was found that the values of gassed T_m were on the whole small compared those of ungassed T_m. Both the resultant C_d and C_m exhibited the low values under the gassed condition in comparison with the ungassed one.

For all systems when the agitation conditions such as the agitation rate, N_{fr}, and the number of impellers, n_i, were varied in electrolyte solutions of different concentrations, C_e, the drag coefficients decreased with increase of the superficial gas velocity, V_s. The dependences of the ratios of gassed coefficients to ungassed ones, C_{dg}/C_{do} and C_{mg}/C_{mo}, characterizing the decrease of the resistance of fluid for the impeller rotation due to aeration, on the agitation conditions were examined. C_{dg}/C_{do} and C_{mg}/C_{mo} decreased with increase of N_{fr}, whereas the coefficient ratios were almost independent of n_i and C_e. The drag coefficients with variation of the aeration and agitation condition in the electrolyte solutions were correlated in the following form:

$$C_d=(0.0024n_i^{0.89})\exp[-(2.3\times0.52)V_s^{0.69}N_{fr}^{0.69}] \quad (11)$$

$$C_m=(0.00032N_{fr}^{-0.06}n_i^{1.00})\exp[-(2.3\times0.31)V_s^{1.07}N_{fr}^{1.07}] \quad (12)$$

The correlation results are shown in Figs 4 and 5 as the relation between C_{dg}/C_{do} and $0.52V_s^{0.69}N_{fr}^{0.69}$ and that between C_{mg}/C_{mo} and $0.31V_s^{1.07}N_{fr}^{1.07}$, respectively. As can be seen from the figures, the observed values of respective drag coefficients were satisfactorily reproduced by Eqs (11) and (12).

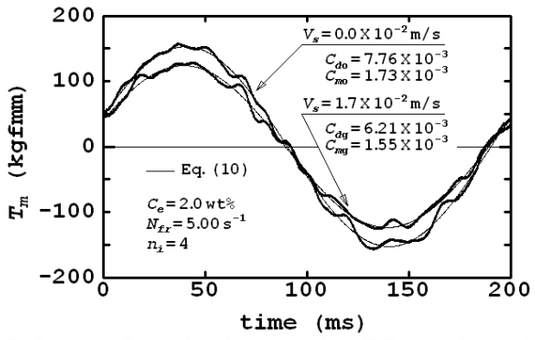

Fig. 3. Time-course of agitation torque, T_m.

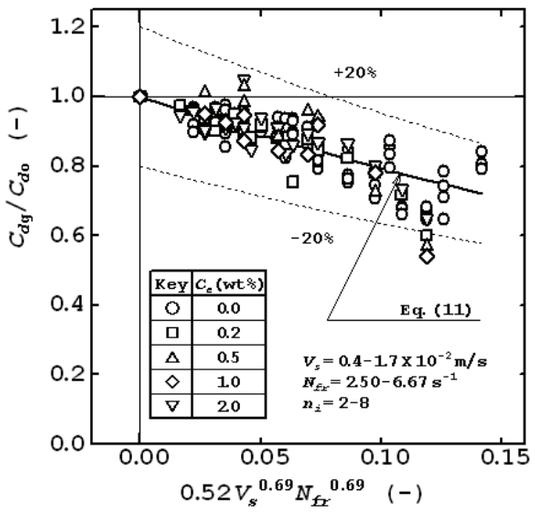

Fig. 4. Relationship between drag coefficient C_{dg}/C_{do} and operating conditions.

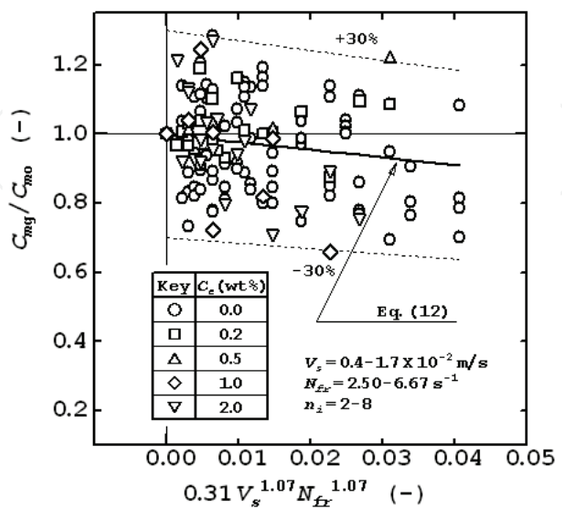

Fig. 5. Relationship between drag coefficient C_{mg}/C_{mo} and operating conditions.

3.2 Power consumption of impeller

The instantaneous power consumption, i.e., the agitation power, P_m, in the cycle of forward-reverse rotation of impeller could be expressed by the following equation as the product of the agitation torque, T_m, [Eq.(10)] and the angular velocity of impeller, ω_i, [Eq.(1)]:

$$P_m=(\rho D_i^5\theta_o^3\omega_{fr}^3)\sin(\omega_{fr}t)[(8C_d/3\pi)\sin(\omega_{fr}t)+(C_m/\theta_o)\cos(\omega_{fr}t)] \quad (13)$$

Using Eq. (13), the time-averaged power consumption, P_{mav}, that is based on the total energy transmitted in one cycle of forward-reverse rotation of impeller is related to the viscous drag coefficient, C_d, as follows:

$$P_{mav}=\oint P_m dt/(2\pi/\omega_{fr})=(4/3\pi)(\rho D_i^5\theta_o^3\omega_{fr}^3)C_d \quad (14)$$

Figure 6 shows an example of the changes in P_m with time. The thin solid line in the figure is for the values calculated from Eq. (13) with the drag coefficients, C_d and C_m, determined experimentally. Agreements between the observed and calculated values were found to be good. According to Eq. (2), the value of P_{mav} was determined by integrating graphically P_m with the time. On the other hand, combined use of Eq. (14) with Eq. (11) enables to calculate P_{mav} as a function of the aeration and agitation conditions such as V_s, N_{fr} and n_i. Figure 7

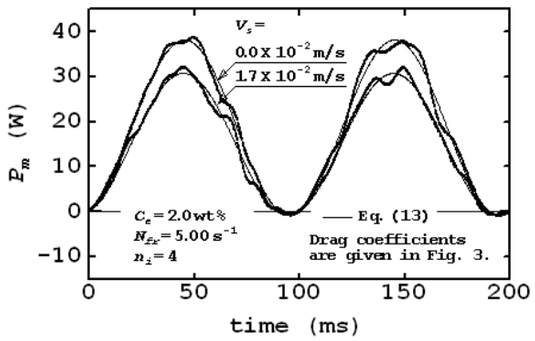

Fig. 6. Time-course of agitation power, P_m.

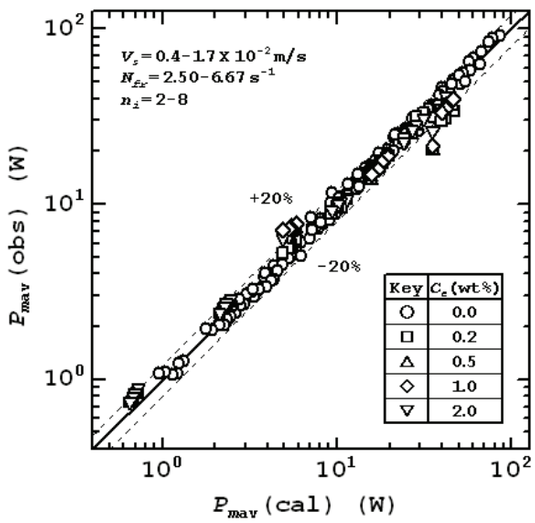

Fig. 7. Comparison of average agitation power, P_{mav}, values observed with those calculated.

compares the $P_{m\mathrm{av}}$ values determined experimentally with those calculated from Eq. (14) used with Eq. (11). These equations reproduced the experimental $P_{m\mathrm{av}}$ values with an accuracy of ±20 % and was demonstrated to be useful for prediction of the values of the power consumption of the forward-reverse rotating impeller.

Equations (11) and (12) indicate that the power consumption of the forward-reverse rotating impeller in liquid phase where gas bubbles are dispersed is independent of the electrolyte concentration. That is, the power characteristics are perceived to be independent of the dispersing gas bubble size which changes depending on the electrolyte concentration in liquid phase. This result, which is observed also for unidirectionally rotating impellers (Bruijn *et al.*, 1974), would be caused by difficulty for the cavities formed behind the blades of impeller to be affected by small sized gas bubbles dispersed in liquid phase.

4. Mass transfer characteristics of forward-reverse agitation vessel

The differences of the volumetric coefficient of mass transfer when the aeration and agitation conditions were varied were investigated in terms of the power input. A total power input was employed as the sum of the aeration and agitation power inputs. The aeration power input defined as the power of isothermal expansion of gas bubbles to their surrounding liquid was calculated from Eq. (3). For the agitation power input, the average power consumption of impeller calculated from Eqs (14) and (11) was used. Figure 8 shows a typical result of the volumetric coefficient, k_La_L, plotted against the total power input per unit mass of liquid, P_{tw}, with the electrolyte concentration, C_e, and the superficial gas velocity, V_s, as parameters. For any system, k_La_L tended to increase almost linearly with P_{tw}. The rate of increase in k_La_L with P_{tw} was practically independent of V_s but differed depending on the conditions with and without electrolyte in liquid phase.

The results for the baffled vessel agitated by the unidirectionally rotating multiple DT impellers examined as a control and those reported by Van't Riet (1979) and Nocentini *et al.* (1993) are also shown in Fig. 8. Although the tendency that the dependence of k_La_L on P_{tw} becomes larger in existence of electrolyte in liquid phase was common to the forward-reverse and unidirectional agitation modes, the dependence for the former mode was larger than that for the latter one. As a result, favorably comparable k_La_L values were obtained in the unbaffled vessel agitated by the forward-reverse rotating impellers.

Presence of electrolytes in liquid phase is known to decrease the rate for gas bubbles to coalesce (Marrucci and Nicodemo, 1967; Zieminski and Whittemore, 1971) and to decrease the size of gas bubbles dispersed in liquid phase (Linek *et al.*, 1970; Robinson and Wilke, 1973; Robinson and Wilke, 1974; Van't Riet, 1979; Hassan and Robinson, 1980; Linek *et al.*, 1987). Decreased size of gas bubbles in liquid phase containing electrolyte causes increase of the gas-liquid interfacial area, a_L, which is further enhanced by the tendency for the gas hold-up to increase with decrease of the bubble size. On the other hand, decrease of the bubble size causes decrease of the liquid-phase mass transfer coefficient, k_L, and then k_L is often considered to be a function of the bubble size (Robinson and Wilke, 1974; Hassan and Robinson, 1980). That is, the volumetric coefficient that is the product of a_L and k_L suffers the two counter influences. In the following sections, the mass transfer parameters such as a_L and k_L are addressed for enhancement of the gas-liquid mass transfer in the forward-reverse agitation vessel to be assessed.

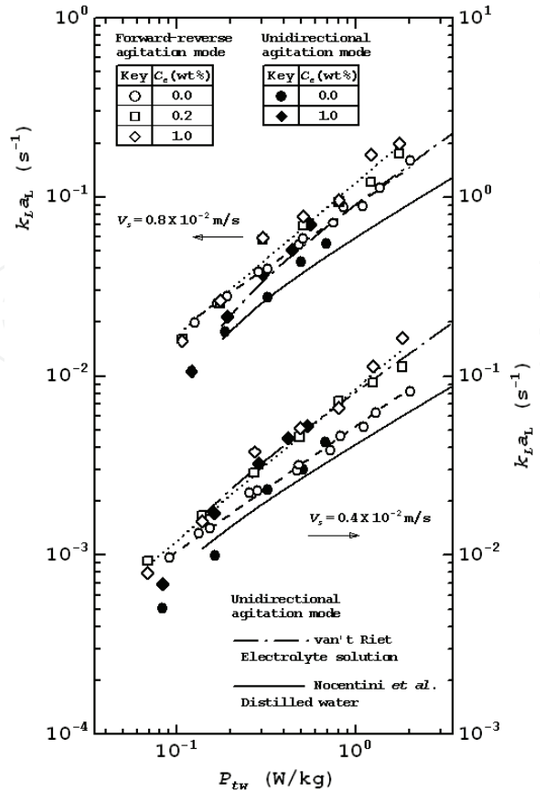

Fig. 8. Comparison of volumetric coefficient, $k_L a_L$, as viewed from change in specific total power input, P_{tw}.

5. Hydrodynamics of forward-reverse agitation vessel

5.1 Mean bubble diameter

The dependence of the size of gas bubbles on aeration and agitation conditions was investigated in terms of the power input. Figure 9 shows a typical relationship between the mean bubble diameter, d_{vs}, and the total power input per unit mass of liquid, P_{tw}, with the electrolyte concentration, C_e, and the superficial gas velocity, V_s, as parameters. For any system, d_{vs} tended to decrease with P_{tw}. The values of d_{vs} at the same level of P_{tw} were almost independent of V_s but differed depending on C_e.

The mean bubble diameter, d_{vs}, was then analyzed with the aeration and agitation conditions. Based on the results shown in Fig. 9, the following functional form was assumed for the empirical equation of d_{vs} with the specific total power input, P_{tw}.

$$d_{vs}=AP_{tw}^{a} \tag{15}$$

The exponent, a, of P_{tw} was obtained from the slope of the straight lines as drawn in Fig. 9. Its value was independent of the electrolyte concentration, C_e. The coefficient, A, changed depending on C_e and its dependence was expressed for the experimental material of this work as follows:

$$A=-1.49C_e^{0.096}+2.95 \tag{16}$$

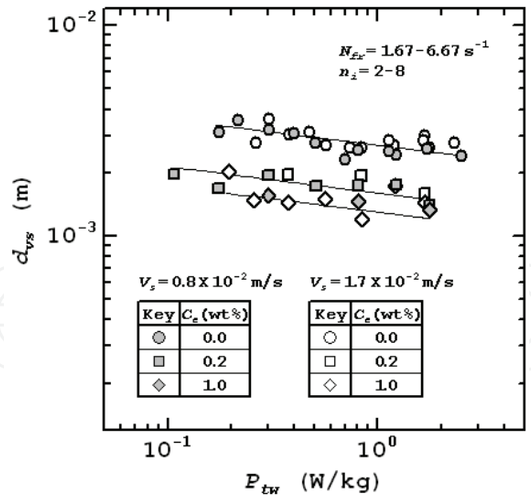

Fig. 9. Relationship between mean bubble diameter, d_{vs}, and specific total power input, P_{tw}.

As a result, the empirical equation of d_{vs} is

$$d_{vs}=(-1.49C_e^{0.096}+2.95)P_{tw}^{-0.12} \quad (17)$$

Figure 10 presents a comparison between d_{vs} values observed and those calculated from Eq. (17). As shown in the figure, d_{vs} could be correlated within approximately 20 %.

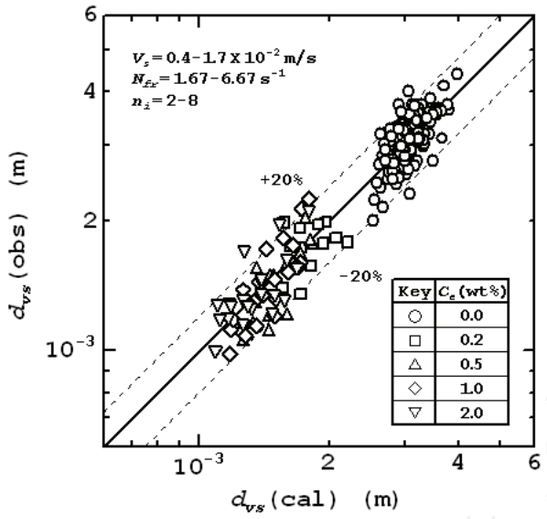

Fig. 10. Comparison of d_{vs} values observed with those calculated.

5.2 Gas hold-up

The dependence of gas hold-up was investigated in relation to the total power input, similarly to that of bubble size. Figure 11 shows a typical relationship between the gas hold-up, ϕ_{gD}, and the total power input per unit mass of liquid, P_{tw}. Although ϕ_{gD} increased with P_{tw}, its values differed depending on the electrolyte concentration, C_e, and the superficial gas velocity, V_s.
The gas hold-up, ϕ_{gD}, was then analyzed with the aeration and agitation conditions. Based on the results shown in Fig. 11, the following functional form was inferred for the empirical equation of ϕ_{gD}.

$$\phi_{gD}=BP_{tw}^{b1}V_s^{b2} \tag{18}$$

The exponent, b1, of the specific total power input, P_{tw}, was obtained from the slope of the straight lines as drawn in Fig. 11. The exponent, b2, of the superficial gas velocity, V_s, was determined from the slope of the cross plots. The coefficient, B, was expressed as a function of the electrolyte concentration, C_e, as follows:

$$B=0.629C_e^{0.27}+1.32 \tag{19}$$

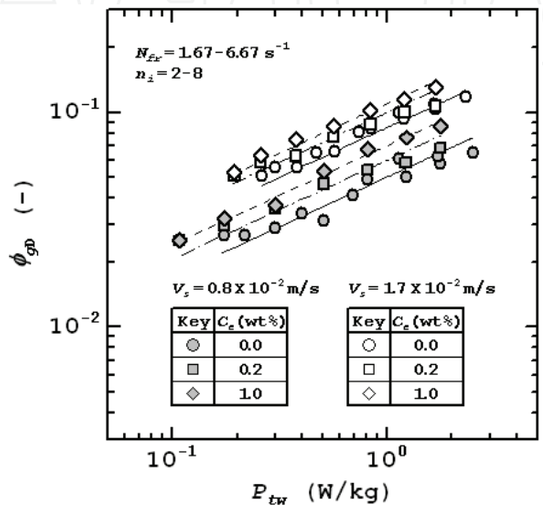

Fig. 11. Relationship between gas hold-up, ϕ_{gD}, and specific total power input, P_{tw}.

Figure 12 shows that ϕ_{gD} could be correlated by the following equation within approximately 30 %.

$$\phi_{gD}=(0.629C_e^{0.27}+1.32)P_{tw}^{0.46}V_s^{0.70} \tag{20}$$

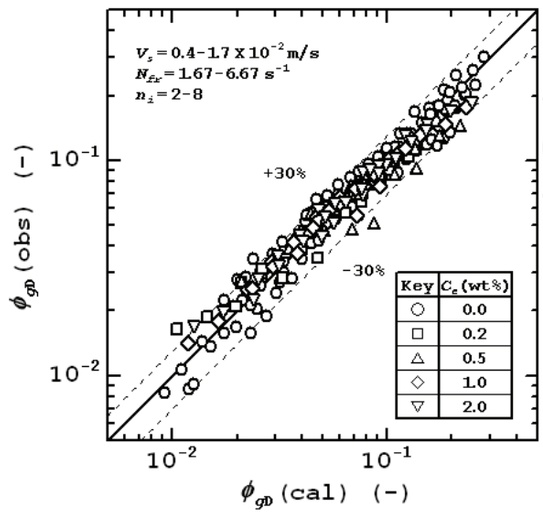

Fig. 12. Comparison of ϕ_{gD} values observed with those calculated.

5.3 Gas-liquid interfacial area

For electrolyte solutions aerated at the velocities ranged in this work, no significant difference in the mean bubble diameter and the gas hold-up determining the magnitude of gas-liquid interfacial area was observed between forward-reverse and conventional agitation vessel. From this, somewhat larger values of volumetric coefficient as illustrated in Fig. 8 in the former vessel may be a reflection of the contribution of forward-reverse rotation of the impeller to increase of the liquid-phase mass transfer coefficient with occurrence of an intensified liquid turbulence in the vicinity of the gas-liquid interface.

6. Mass transfer consideration

6.1 Analysis of mass transfer coefficient

Calderbank and Moo-Young (1961) first examined the liquid-phase mass transfer coefficient, k_L, as a function of the size of particles dispersed in a conventional baffled vessel agitated by a unidirectionally rotating impeller. Subsequently, they elucidated the mechanism of mass transfer by comparing the results with two typical theoretical predictions for single particle. They recommended applications of Froessling's laminar boundary layer theory (Froessling, 1938) and Higbie's penetration theory (Higbie, 1935) to elucidate the respective mechanisms of gas-liquid mass transfer for small (diameter, d_b<0.5 mm) and large (d_b>2.5 mm) gas bubbles. These two theories express the mass transfer characteristics in relation to the rising velocity of gas bubble, V_b, as follows.

Froessling equation:

$$k_L=(2D_L/d_b)+0.55\rho^{1/6}\mu^{-1/6}V_b^{1/2}d_b^{-1/2}D_L^{2/3} \tag{21}$$

Higbie equation:

$$k_L=(2/\pi^{1/2})[D_L/(d_b/V_b)]^{1/2} \tag{22}$$

In these equations, ρ is the liquid density, μ is the liquid viscosity, and D_L is the liquid-phase diffusivity.

The relationship between the liquid-phase mass transfer coefficient, k_L, and the gas bubble size was investigated for the unbaffled vessel agitated by the forward-reverse rotating impellers. Figure 13 shows the plot of k_L against the volume-surface mean bubble diameter, d_{vs}, which is a parameter that characterizes the size of a swarm of gas bubbles. The k_L values for the baffled vessel agitated by the unidirectionally rotating multiple DT impellers (conventional agitation vessel) examined as a control and those reported by Calderbank and Moo-Young (1961) are also shown. The dotted lines for comparison indicate the two theoretical predictions for single bubble with the diameter d_b. Here, the values of V_b that are necessary for calculations from Eqs (21) and (22) were estimated using the equation presented by Tadaki and Maeda (1961). The values of d_{vs} observed in the forward-reverse agitation vessel ranged from 1 to 4 mm. Regarding the difference of k_L caused by the bubble size, the two regions with the boundary of 2.5 mm diameter was common to the forward-reverse and conventional agitation vessel. As can be seen from the figure, k_L values for forward-reverse agitation vessel were noticeably different from those for conventional one. That is, k_L came to exhibit higher values than those by Calderbank and Moo-Young, with the maximum difference being about three times, when the agitation rate, N_{fr}, was increased. For such a peculiar difference of k_L with N_{fr} for bubbles of similar sizes, consideration is

necessary in terms of hydrodynamic parameters, taking into account not only the mean bubble diameter but also other important variables such as the rising velocity of a swarm of gas bubbles that changes depending on the gas hold-up. Specifically, examination is required of the mass transfer characteristics as viewed from change in the Reynolds number, which is a parameter characterizing the liquid flow around gas bubble.

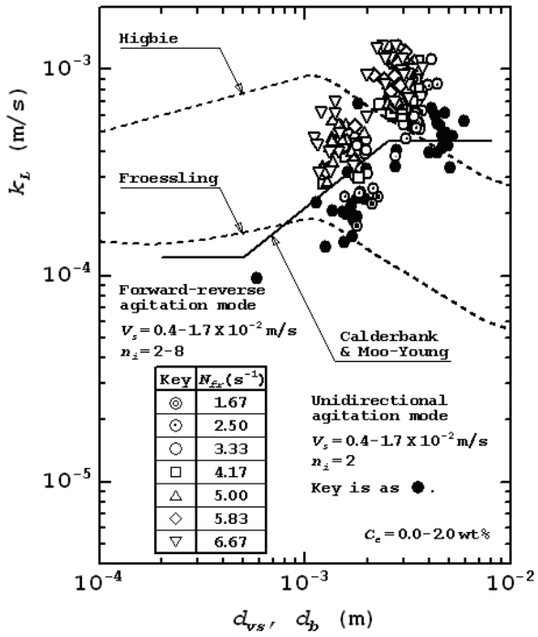

Fig. 13. Relationship between mass transfer coefficient, k_L, and gas bubble size.

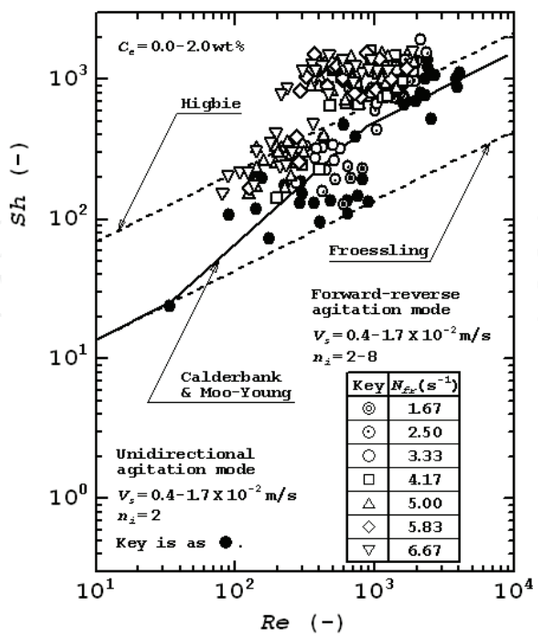

Fig. 14. Relationship between *Sh* and *Re*.

6.2 Correlation of Sherwood number

Mass transfer characteristics from bodies in a steadily flowing fluid or from bodies moving steadily in a fluid at rest are expressible using dimensionless terms that characterize transport phenomena involving the size and velocity of the body and the physical properties of the fluid. This has led many researchers to determine the functional form in the following correlation form with dimensionless terms and to evaluate the mass transfer characteristics, i.e., the mechanism of mass transfer, of the intended gas-liquid contactors by comparing results obtained experimentally with the theoretical predictions.

$$Sh=\text{func.}\ (Re, Sc) \tag{23}$$

where Sh is the Sherwood number, Re is the Reynolds number and Sc is the Schmidt number. These dimensionless terms can be given in the following forms, respectively, when the overall mass transfer coefficient for the single bubble with diameter, d_b, and rising velocity, V_b, is approximated by the liquid-phase mass transfer coefficient, k_L.

$$Sh=k_L d_b/D_L \tag{24}$$

$$Re=\rho V_b d_b/\mu \tag{25}$$

$$Sc=\mu/\rho D_L \tag{26}$$

The Froessling and Higbie equations mentioned above are expressed in the forms of Eq. (23), respectively, as
Froessling equation:

$$Sh=2+0.55Re^{1/2}Sc^{1/3} \tag{27}$$

Higbie equation:

$$Sh=(2/\pi^{1/2})Re^{1/2}Sc^{1/2} \tag{28}$$

To examine the relationship between the non-dimensionalized k_L, Sh, and Re for the unbaffled vessel agitated by the forward-reverse rotating impellers, d_b in the dimensionless terms was replaced by the mean diameter of a swarm of gas bubbles, d_{vs}, and d_{vs} was regarded as a characteristic length. The mean rising velocity of a swarm of gas bubbles, V_{bs}, as calculated from the following equation when the distribution of gas hold-up was assumed to be uniform on any horizontal section within the vessel, was used for V_b necessary to calculate Re:

$$V_{bs}=V_s/\phi_{g\mathrm{D}} \tag{29}$$

where V_s is the superficial gas velocity. $\phi_{g\mathrm{D}}$ is the gas hold-up and the values determined as the average within the vessel were used for calculation from Eq. (29).
Figure 14 shows the relationship between Sh and Re for the forward-reverse agitation vessel. The Sh values for the conventional agitation vessel as a control and those by Calderbank and Moo-Young (1961) are also shown in comparison with the theoretical predictions for single bubble. For the mean bubble diameter, d_{vs}, larger than 2.5 mm, the Sh values for the conventional agitation vessel more closely resembled the values calculated from the Higbie equation than those calculated from the Froessling equation. For d_{vs} smaller than 2.5 mm, decrease of Sh with decrease of Re was remarkable, with Sh exhibiting the values that are

intermediary between those from the Higbie and Froessling equations. This fact suggests that the contribution of liquid flow to the mass transfer is reduced considerably if the internal circulation within gas bubble is prevented from becoming fully developed through decreased rising velocity of gas bubble that is attributable to its decreased size, namely, smaller inertial force of rising motion of gas bubble (Tadaki and Maeda, 1963; Sideman *et al.*, 1966). The relationship between *Sh* and *Re* for the forward-reverse agitation vessel under the condition of lower agitation rates exhibited the same tendency as that for the conventional agitation vessel, as shown in the figure. That is, *Sh* under such conditions increased approximately in proportion to $Re^{0.5}$, according to the Higbie equation, for d_{vs} larger than 2.5 mm, and in proportion to *Re* for d_{vs} smaller than 2.5 mm. When the agitation rate, N_{fr}, is increased, an increased gas hold-up and a decreased mean bubble diameter cause *Re*, as defined by Eq. (25), to have lower values. Under the conditions as *Re* decreased or N_{fr} increased, *Sh* for the forward-reverse agitation vessel tended to exhibit higher values than those for the conventional agitation vessel. For the forward-reverse agitation vessel, i.e., unsteady bulk flow type contactor, the dependence of *Sh* on *Re*, characteristically different from that for the conventional agitation vessel, i.e., steady bulk flow type contactor, suggests an effect of unsteady oscillating flow produced by forward-reverse rotation of the impeller on enhancement of the mass transfer. For quantifying *Sh* in this gas-liquid agitation system, further consideration is necessary taking into account a parameter characterizing the unsteady oscillating flow, in addition to *Re* as a measure of the liquid flow around gas bubble.

Many theoretical and experimental studies on the mass transfer between gas bubble and its surrounding liquid in a steady state have given the relation in the form of Eq. (23) as an equation that expresses gas-liquid mass transfer characteristics. The dimensionless terms in Eq. (23) are obtained by non-dimensionalizing the equation of motion determining the liquid flow around gas bubble, the diffusion equation determining the mass transfer between gas bubble and its surrounding liquid and the mass balance equation, respectively, under a condition of steady liquid flow. On the other hand, the time-dependent term in the equation of motion should be considered for analysis of the liquid flow around gas bubble when gas bubble rises in liquid with unsteady oscillating flow produced by forward-reverse rotation of the impeller. The dimensionless terms, the Sherwood number (*Sh*), the Reynolds number (*Re*), the Strouhal number (*St*), and the Schmidt number (*Sc*), which are necessary to express the unsteady mass transfer phenomena, are all derived based on the equation of motion that is non-dimensionalized under a condition of unsteady liquid flow, the dimensionless diffusion equation and the dimensionless mass balance equation. Therefore, *Sh* in this gas-liquid agitation system is given as a function of *Re*, *St* and *Sc*.

$$Sh=\text{func.}\,(Re, St, Sc) \tag{30}$$

Definitions of *Sh*, *Re* and *Sc* are mentioned above; *St* is defined for single gas bubble as

$$St=fd_b/V_b \tag{31}$$

The diameter, d_b, and the velocity, V_b, for *St* were identical to those for *Re*. The frequency of forward-reverse rotation of impeller, N_{fr}, was taken as a characteristic frequency, *f*.

The experimental results shown in Fig. 14 suggest that the two coexisting liquid flows affect *Sh* in a form of their superposition. Then, the degree of effect would be determined by the relative magnitude of *Re* characterizing the steady slip flow of surrounding liquid with the

rising motion of gas bubble and *St* characterizing the unsteadily oscillating flow of liquid around gas bubble by forward-reverse rotation of the impeller. Furthermore, a value of 1/2, which many researchers (Calderbank, 1959; Yagi and Yoshida, 1975; Nishikawa *et al.*, 1981; Panja and Phaneswara Rao, 1993; Zeybek *et al.*, 1995; Linek *et al.*, 2005) have used for a swarm of gas bubbles in a relatively large size range, is assumed to be adoptable as an exponent indexing the dependence of *Sh* on *Sc*. Consequently, Eq. (30) can be concretized in the following functional form:

$$Sh=[\text{func. }(Re)+CSt^{c}]Sc^{1/2} \tag{32}$$

Therein, func. (*Re*) is based on the relation by Calderbank and Moo-Young (1961), which differs depending on the range of mean bubble diameter, as illustrated in Fig. 14, and is given by the following equations.
d_{vs}<2.5 mm:

$$\text{func. }(Re)=0.0544Re^{0.90} \tag{33}$$

d_{vs}>2.5 mm:

$$\text{func. }(Re)=(2/\pi^{1/2})Re^{1/2} \tag{34}$$

The term in the bracket on the right side of Eq. (32) is expected to express the combined effect of the two liquid flows, namely, the relative influence of the steady slip flow and the unsteady oscillating flow, on the gas-liquid mass transfer.
On the basis of Eq. (32), the relationship between $Sh/Sc^{1/2}$-func. (*Re*) and *St* was examined. From the slope of the line and the intercept on the axis in the logarithmic plot, the empirical constants, c and C, were determined for the respective ranges with d_{vs}=2.5 mm as a boundary, and then the following correlation equations were obtained.
d_{vs}<2.5 mm:

$$Sh=[0.0544Re^{0.90}+10.0St^{0.10}]Sc^{1/2} \tag{35}$$

d_{vs}>2.5 mm:

$$Sh=[(2/\pi^{1/2})Re^{1/2}+180St^{0.79}]Sc^{1/2} \tag{36}$$

The result of correlation of *Sh* is shown in Fig. 15. As shown in the figure, *Sh* was correlated with *Re* and *St* with an accuracy of ±40 %. A positive dependence of *Sh* on *St* is considered to indicate that the time-dependence in the flow of liquid around gas bubble, namely, the inertial force caused by the local acceleration produced by forward-reverse rotation of the impeller, contributes to enhancement of the gas-liquid mass transfer. This contribution could be significant when the velocity gradients in the flow of the surrounding liquid, namely, the inertial force caused by the convective acceleration produced by the rising motion of gas bubble, is smaller. Equations (35) and (36) are applicable when *Re* is 100-2300, that is, the flow of liquid around gas bubble is practically turbulent, for *St* of up to 0.20.

6.3 Correlation of volumetric coefficient

Correlation of the volumetric coefficient of gas-liquid mass transfer was then made based on the experimental results mentioned above. The volumetric coefficient, k_La_D, based on the gassed liquid volume was intended for correlation. k_La_D is the product of the liquid-phase mass transfer coefficient, k_L, and the gas-liquid interfacial area, a_D.

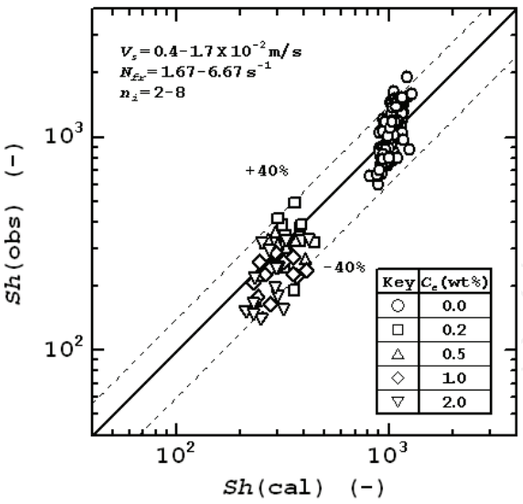

Fig. 15. Comparison of *Sh* values observed with those calculated.

$$k_L a_D = (k_L)(a_D) \tag{37}$$

It is noteworthy that a_D depends on the volume-surface mean bubble diameter, d_{vs}, and the gas hold-up, ϕ_{gD}, according to Eq. (5). Substituting Eq. (5) into Eq. (37) yields the following equation, which gives the relation between $k_L a_D$ and the mass transfer parameters.

$$k_L a_D = 6\phi_{gD} k_L / d_{vs} \tag{38}$$

The empirical equations for d_{vs} and ϕ_{gD} are given respectively as Eqs (17) and (20). In addition, the values of k_L are predicted by combined use of Eq. (35) or (36) and Eqs (17) and (20). Figure 16 shows the observed $k_L a_D$ values along with those obtained by substituting the calculated values of the mass transfer parameters into Eq. (38). As shown in the figure, $k_L a_D$ could be correlated with an accuracy of ±35 %. Moreover, Eqs (17) and (20) are relations in terms of the specific power input and Eqs (35) and (36) are a dimensionless relation. As demonstrated by some researchers (Van't Riet, 1979), the relations based on such correlation forms are expected to be useful for operational design, i.e., scale-up, of the apparatus.

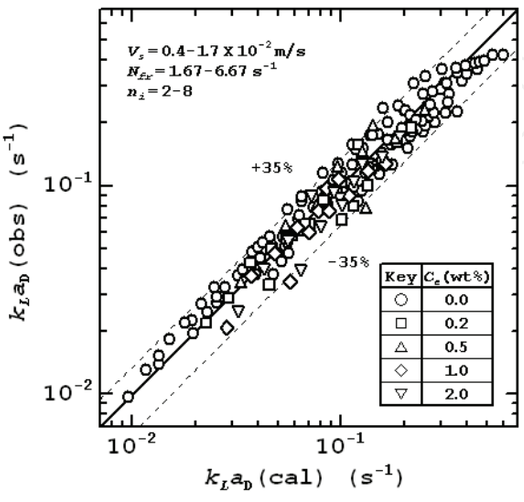

Fig. 16. Comparison of $k_L a_D$ values observed with those calculated.

7. Conclusion

For a gas-sparged, unbaffled vessel agitated by the forward-reverse rotating multiple impellers, the volumetric coefficient of oxygen transfer in air-electrolyte solution systems was correlated in relation to mass transfer parameters such as the mean bubble diameter, gas hold-up and liquid-phase mass transfer coefficient. The effects of gassing rate, agitation rate and the number of impellers on the bubble diameter and hold-up were examined. The empirical equations were obtained to predict their values as a function of the specific total power input, superficial gas velocity and electrolyte concentration in liquid phase. The difference of liquid-phase mass transfer coefficient, non-dimensionalized in a form of the Sherwood number, was related to changes of the Reynolds number and Strouhal number characterizing the mass transfer between gas bubble and its surrounding liquid in the unsteadily oscillating flow.

8. References

Bruijn, W., Van't Riet, K. and Smith, J. M. (1974). Power consumption with aerated Rushton turbines. *Trans. Inst. Chem. Engrs*, Vol. 52, pp. 88-104

Calderbank, P. H. (1959). Physical rate processes in industrial fermentation, Mass transfer coefficient in gas-liquid contacting with mechanical agitation. *Trans. Inst. Chem. Engrs*, Vol. 37, pp. 173-185

Calderbank, P. H. and Moo-Young, M. B. (1961). The continuous phase heat and mass-transfer properties of dispersions. *Chem. Eng. Sci.*, Vol. 16, pp. 39-54

Chapman, C. M., Gibilaro, L. G. and Nienow, A. W. (1982). A dynamic response technique for the estimation of gas-liquid mass transfer coefficients in a stirred vessel. *Chem. Eng. Sci.*, Vol. 37, pp. 891-896

Froessling, N. (1938). On the vaporization of a falling drop. *Gerlands Beitr Geophys*, Vol. 52, pp. 170-216

Hassan, I. T. M. and Robinson, C. W. (1980). Mass transfer coefficient in mechanically agitated gas-aqueous electrolyte dispersions. *Can. J. Chem. Eng.*, Vol. 58, pp. 198-205

Higbie, R. (1935). The rate of absorption of a pure gas into a still liquid during short periods of exposure. *Trans. Am. Inst. Chem. Engrs*, Vol. 31, pp. 365-388

Linek, V., Mayrhoferova, J. and Mosnerova, J. (1970). The influence of diffusivity on liquid phase mass transfer in solutions of electrolytes. *Chem. Eng. Sci.*, Vol. 25, pp. 1033-1045

Linek, V., Vacek, V. and Benes, P. (1987). A critical review and experimental verification of the correct use of the dynamic method for the determination of oxygen transfer in aerated agitated vessels to water, electrolyte solutions and viscous liquids. *Chem. Eng. J.*, Vol. 34, pp. 11-34

Linek, V., Kordac, M. and Moucha, T. (2005). Mechanism of mass transfer from bubbles in dispersions, mass transfer coefficients in stirred gas-liquid reactor and bubble column. *Chem. Eng. Processing*, Vol. 44, pp. 121-130

Marrucci, G. and Nicodemo, L. (1967). Coalescence of gas bubbles in aqueous solutions of inorganic electrolytes. *Chem. Eng. Sci.*, Vol. 22, pp. 1257-1265

Nienow, A. W. (1990). Gas dispersion performance in fermenter operation. *Chem. Eng. Prog.*, No. 2, pp. 61-71

Nishikawa, M., Nakamura, M. and Hashimoto, K. (1981). Gas absorption in aerated mixing vessels with non-Newtonian liquid. *J. Chem. Eng. Japan*, Vol. 14, pp. 227-232

Nocentini, M., Fajner, D., Pasquali, G. and Magelli, F. (1993). Gas-liquid mass transfer and holdup in vessels stirred with multiple Rushton turbines: Water and water-glycerol solutions. *Ind. Eng. Chem. Res.*, Vol. 32, pp. 19-26

Panja, N. C. and Phaneswara Rao, D. (1993). Measurement of gas-liquid parameters in a mechanically agitated contactor. *Chem. Eng. J.*, Vol. 52, pp. 121-129

Robinson, C. W. and Wilke, C. R. (1973). Oxygen absorption in stirred tanks, A correlation for ionic strength effects. *Biotechnol. Bioeng.*, Vol. 15, pp. 755-782

Robinson, C. W. and Wilke, C. R. (1974). Simultaneous measurement of interfacial area and mass transfer coefficients for a well-mixed gas dispersion in aqueous electrolyte solutions. *AIChE J.*, Vol. 20, pp. 285-294

Sideman, S., Hortacsu, O. and Fulton, J. W. (1966). Mass transfer in gas-liquid contacting systems. *Ind. Eng. Chem.*, Vol. 58, pp. 32-47

Tadaki, T. and Maeda, S. (1961). On the shape and velocity of single air bubbles rising in various liquids. *Kagaku Kogaku*, Vol. 25, pp. 254-264

Tadaki, T. and Maeda, S. (1963). On the CO_2 desorption in the gas bubble column. *Kagaku Kogaku*, Vol. 27, pp. 808-814

Takahashi, K. (1994). *Fluid Mixing Techniques for New Materials*, p. 143, IPC Publications Co., Ltd., Tokyo

Tanaka, H. and Ueda, K. (1975). Design of a jar fermentor for filamentous microorganisms. *J. Ferment. Technol.*, Vol. 53, pp. 143-150

Van't Riet, K. (1979). Review of measuring methods and results in nonviscous gas-liquid mass transfer in stirred vessels. *Ind. Eng. Chem. Process Des. Dev.*, Vol. 18, pp. 357-364

Warmoeskerken, M. M. C. G. and Smith, J. M. (1985). Flooding of disc turbines in gas-liquid dispersions, A new description of the phenomenon. *Chem. Eng. Sci.*, Vol. 40, pp. 2063-2071

Yagi, H. and Yoshida, F. (1975). Gas absorption by Newtonian and non-Newtonian fluids in sparged agitated vessels. *Ind. Eng. Chem. Process Des. Dev.*, Vol. 14, pp. 488-493

Yoshida, M., Kitamura, A., Yamagiwa, K. and Ohkawa, A. (1996). Gas hold-up and volumetric oxygen transfer coefficient in an aerated agitated vessel without baffles having forward-reverse rotating impellers. *Can. J. Chem. Eng.*, Vol. 74, pp. 31-39

Yoshida, M., Ito, A., Yamagiwa, K., Ohkawa, A., Abe, M., Tezura, S. and Shimazaki, M. (2001). Power characteristics of unsteadily forward-reverse rotating impellers in an unbaffled aerated agitated vessel. *J. Chem. Technol. Biotechnol.*, Vol. 76, pp. 383-392

Yoshida, M., Watanabe, M., Yamagiwa, K., Ohkawa, A. Abe, M., Tezura, S. and Shimazaki, M. (2002). Behaviour of gas-liquid mixtures in an unbaffled reactor with unsteadily forward-reverse rotating impellers. *J. Chem. Technol. Biotechnol.*, Vol. 77, pp. 678-684

Yoshida, M., Akiho, M., Nonaka, K., Yamagiwa, K., Ohkawa, A. and Tezura, S. (2005). Mixing and mass transfer characteristics of an unbaffled aerated agitation vessel with unsteadily forward-reverse rotating multiple impellers. *Lat. Amer. Appl. Research*, Vol. 35, pp. 37-42

Zeybek, Z., Oguz, H. and Berber, R. (1995). Gas/liquid mass transfer in concentrated polymer solutions. *Chem. Eng. Res. Des.*, Vol. 73, pp. 622-626

Zieminski, S. A. and Whittemore, R. C. (1971). Behavior of gas bubbles in aqueous electrolyte solutions. *Chem. Eng. Sci.*, Vol. 26, pp. 509-520

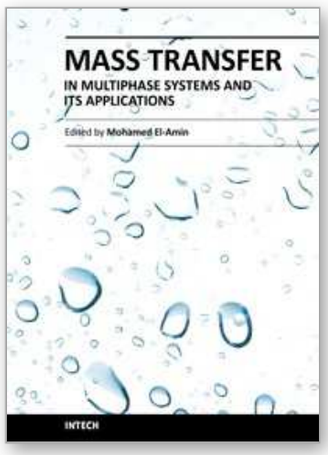

Mass Transfer in Multiphase Systems and its Applications
Edited by Prof. Mohamed El-Amin

ISBN 978-953-307-215-9
Hard cover, 780 pages
Publisher InTech
Published online 11, February, 2011
Published in print edition February, 2011

This book covers a number of developing topics in mass transfer processes in multiphase systems for a variety of applications. The book effectively blends theoretical, numerical, modeling and experimental aspects of mass transfer in multiphase systems that are usually encountered in many research areas such as chemical, reactor, environmental and petroleum engineering. From biological and chemical reactors to paper and wood industry and all the way to thin film, the 31 chapters of this book serve as an important reference for any researcher or engineer working in the field of mass transfer and related topics.

INTECH
open science | open minds

InTech Europe
University Campus STeP Ri
Slavka Krautzeka 83/A
51000 Rijeka, Croatia
Phone: +385 (51) 770 447
Fax: +385 (51) 686 166
www.intechopen.com

InTech China
Unit 405, Office Block, Hotel Equatorial Shanghai
No.65, Yan An Road (West), Shanghai, 200040, China
中国上海市延安西路65号上海国际贵都大饭店办公楼405单元
Phone: +86-21-62489820
Fax: +86-21-62489821

IntechOpen